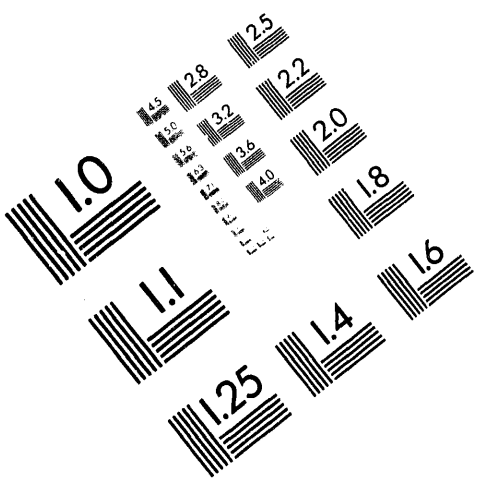

Association for Information and Image Management
1100 Wayne Avenue, Suite 1100
Silver Spring, Maryland 20910
301/587-8202

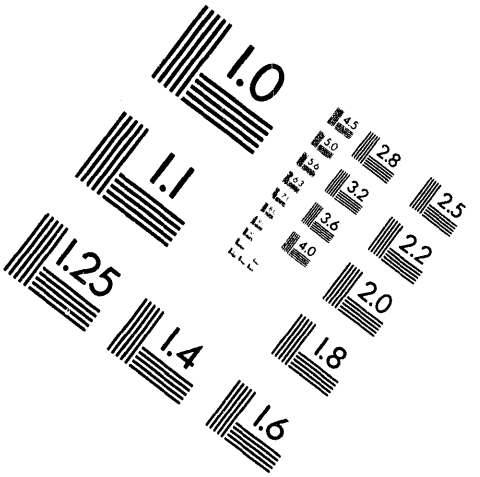

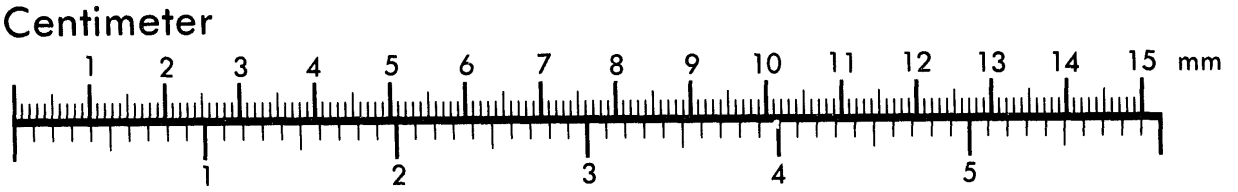

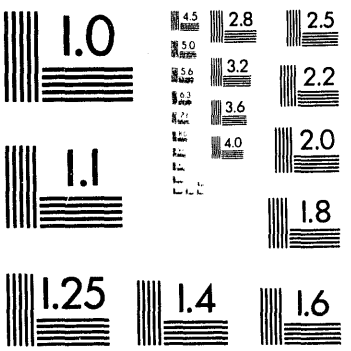

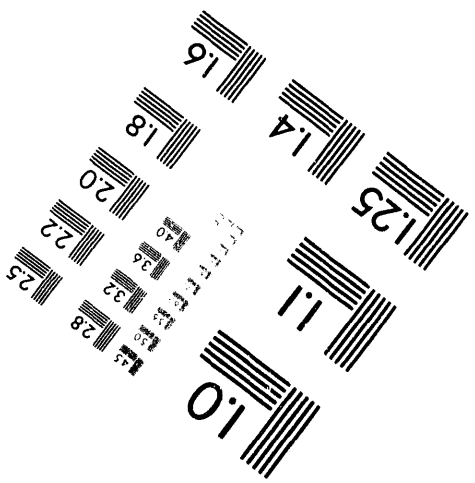

MANUFACTURED TO AIIM STANDARDS
BY APPLIED IMAGE, INC.

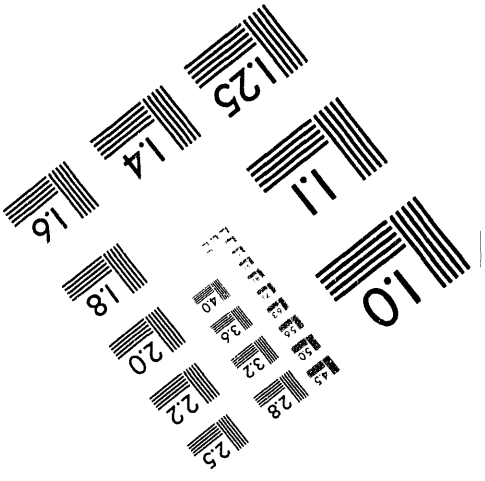

1 of 1

Conf-9307169--2

GA–A21368
JET–P(93)75

INVESTIGATIONS OF VH–MODE IN DIII–D AND JET

by

C.M. GREENFIELD, B. BALET, K.H. BURRELL, M.S. CHU, J.G. CORDEY, J.C. DeBOO, N. DELIYANAKIS, E.J. DOYLE, R.J. GROEBNER, G.L. JACKSON, S. KONOSHIMA, D.P. O'BRIEN, L. PORTE, C.L. RETTIG, T.H. OSBORNE, H. St. JOHN, A.C.C. SIPS, G.M. STAEBLER, E.J. STRAIT, P.M. STUBBERFIELD, T.S. TAYLOR, S.J. THOMPSON, K. THOMSEN, A.D. TURNBULL, and THE JET AND DIII–D TEAMS

SEPTEMBER 1993

GENERAL ATOMICS

DISCLAIMER

GA–A21368
JET–P(93)75

INVESTIGATIONS OF VH–MODE IN DIII–D AND JET

by

C.M. GREENFIELD, B. BALET,* K.H. BURRELL, M.S. CHU, J.G. CORDEY,* J.C. DeBOO, N. DELIYANAKIS,* E.J. DOYLE,** R.J. GROEBNER, G.L. JACKSON, S. KONOSHIMA,*** D.P. O'BRIEN,* L. PORTE,* C.L. RETTIG,** T.H. OSBORNE, H. St. JOHN, A.C.C. SIPS,* G.M. STAEBLER, E.J. STRAIT, P.M. STUBBERFIELD,* T.S. TAYLOR, S.J. THOMPSON, K. THOMSEN,* A.D. TURNBULL, and THE JET AND DIII–D TEAMS

This is a preprint of an invited paper presented at the 20th EPS Conference on Controlled Fusion and Plasma Physics, July 26–30, 1993, Lisboa, Portugal, and to be printed in a special issue of *Plasma Physics and Controlled Fusion.*

Work supported by
U.S. Department of Energy
Contract DE–AC03–89ER51114 and
Grants DE–FG03–92ER54150 and DE–FG03–86ER–52126

*JET Joint Undertaking
**University of California at Los Angeles
***Japan Atomic Energy Research Institute

General Atomics Projects 3466, 3938, and 3940
SEPTEMBER 1993

GENERAL ATOMICS

Investigations of VH-mode in DIII-D and JET

C M Greenfield♮, B Balet†, K H Burrell♮, M S Chu♮, J G Cordey†, J C DeBoo♮, N Deliyanakis†, E J Doyle‡, R J Groebner♮, G L Jackson♮, S. Konoshima♭, D P O'Brien†, L Porte†, C L Rettig‡, T H Osborne♮, H St. John♮, A C C Sips†, G M Staebler♮, E J Strait♮, P M Stubberfield†, T S Taylor♮, S J Thompson♮, K Thomsen†, A D Turnbull♮ and The JET and DIII-D Teams

♮ General Atomics, San Diego, California, USA

† JET Joint Undertaking, Abingdon, Oxon, UK

‡ University of California, Los Angeles, California, USA

♭ Japan Atomic Energy Research Institute, Japan

Abstract. The VH-mode regime of high confinement has been observed in both DIII-D and JET. VH-mode is characterized by thermal confinement twice that seen in H-mode, with the edge transport barrier penetrating deeper into the plasma. Two mechanisms have been identified as important in achieving this high level of confinement. Expansion of the $\vec{E} \times \vec{B}$ velocity shear turbulence suppression zone is important in allowing reductions in local transport, while access to the second ballooning stability regime in the edge allows avoidance or elimination of ELMs which impede the confinement improvement. The high performance phase of these discharges is usually terminated by an MHD event which removes energy from a large portion of the plasma cross-section, and is followed by an H-mode phase.

Keywords. Fusion; tokamak; confinement; transport; stability; VH-mode; JET; DIII-D.

1. Introduction

The VH-mode regime of high energy confinement was first identified in DIII-D following the initial boronization of the vessel (Jackson *et al.*, 1991; Jackson *et al.*, 1992; Greenfield *et al.*, 1992; Taylor *et al.*, 1993; Osborne *et al.*, 1993). This regime is characterized by thermal confinement which reaches levels up to 2.4 times the JET/DIII-D ELM-free H-mode scaling relation (figure 1) (Schissel *et al.*, 1991), and in excess of 4 times the ITER-89P (Yushmanov *et al.*, 1990) L-mode scaling. For some time, discharges with confinement well in excess of twice L-mode have been observed in JET (The JET Team, 1989). Recently, it has been shown that many of these discharges have characteristics similar to the VH-mode (Deliyanakis *et al.*, 1993; Balet *et al.*, 1993), in particular most of the Preliminary Tritium Experiment (PTE) discharges (The JET Team, 1992). VH-mode plasmas have exhibited high performance

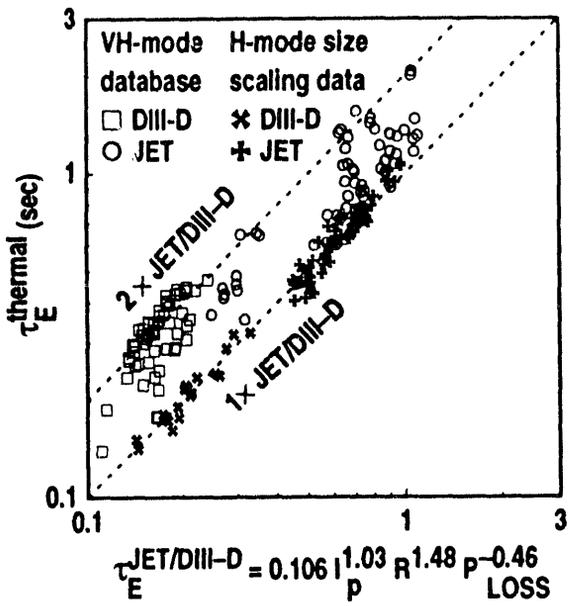

Figure 1. Thermal confinement in VH-mode can exceed twice that in H-mode. The "H-mode size scaling data" was used to fit the JET/DIII-D ELM-free H-mode scaling relation (Schissel *et al.*, 1991), which is shown on the abscissa. The "VH-mode data-base" contains both H- and VH-mode discharges.

commensurate with the high confinement. In each device, the highest fusion triple product $n_D(0)T_i(0)\tau_E^{THERMAL}$ was obtained during VH-mode: 4×10^{20} m^{-3}·keV·sec in DIII-D and 9×10^{20} m^{-3}·keV·sec in JET.

VH-mode discharges are characterized by confinement which rises after a second transition following the L–H transition. Unlike the L–H transition, this is not a sudden transition, but rather a more gradual improvement which can develop over hundreds of milliseconds. Although the transport characteristics often begin improving almost immediately following the L–H transition, there is usually some mechanism which impedes the development of improved confinement. In DIII-D, the improvement is usually delayed by fluctuation bursts (see section 3) known as momentum transfer events (MTEs) (Osborne *et al.*, 1993), which are eventually reduced or eliminated by the development of a broadened region of high radial electric field shear. In JET, the delay is usually caused by ELMs, which last until the plasma edge gains access to the second stable regime to ideal ballooning modes. The elimination of the MTEs or ELMs, and the corresponding confinement increase, are referred to here as the H–VH transition.

The plasma shape is found to be an important factor in obtaining the VH-mode mode in DIII-D (figure 2). High triangularity double-null plasmas are most likely to obtain the VH-mode. This is believed to be because such shapes always have access to the second stable regime to ideal ballooning modes, regardless of the edge current. In JET, no dependence on shape has been identified, probably because experiments in JET rely on the development of high edge bootstrap currents to access the second regime and terminate the ELMing phase.

Confinement generally improves until it reaches a level of approximately twice that predicted by JET/DIII-D scaling. The high performance phase is often terminated by an MHD event. This event is related to both high normalized beta $\beta_N = \beta_T/(I_P/aB_T)$ and high edge current density. In certain discharges in which β_N is kept sufficiently low by limiting the heating power, the termination has either been delayed or eliminated.

In this paper, we will describe the "recipes" for obtaining, and the characteristics of, the VH-mode, as seen in both DIII-D and JET (section 2). Two mechanisms have been identified as playing a role in the improved confinement of VH-mode (section 3): expansion of the $\vec{E} \times \vec{B}$ velocity shear turbulence suppression zone, and expansion of the region with access to the second ballooning stability regime. We will then discuss the termination (section 4). Finally, we will summarize the understanding of the VH-mode as determined from a study of the behavior of both devices (section 5).

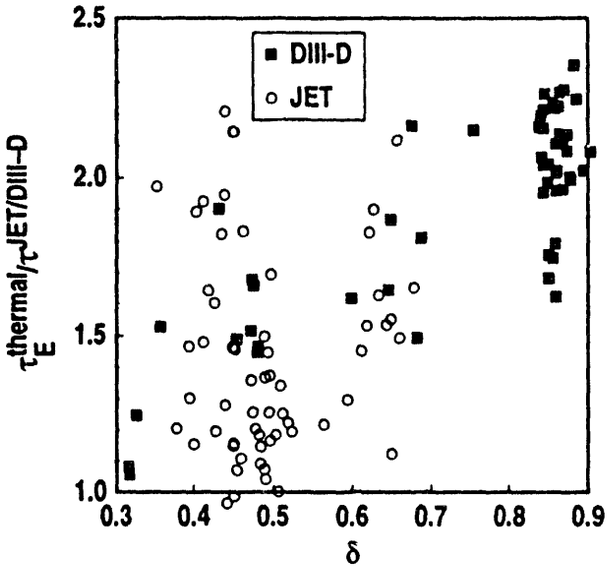

Figure 2. VH-mode confinement enhancement in DIII-D increases with plasma triangularity δ. No such dependency is seen from the JET data.

2. Characteristics of VH-mode

Although the behavior of the two devices are very similar during the VH-mode phase, the time histories leading up to the transition are very different. In the usual "recipe" for VH-mode in DIII-D (figure 3), the plasma is diverted early in the discharge, during the current ramp-up. Typically, the neutral beam power is applied all at once, resulting in a very short ($\sim$ 50 msec) L-mode phase, followed by the L–H transition and an ELM-free H-mode. The second transition

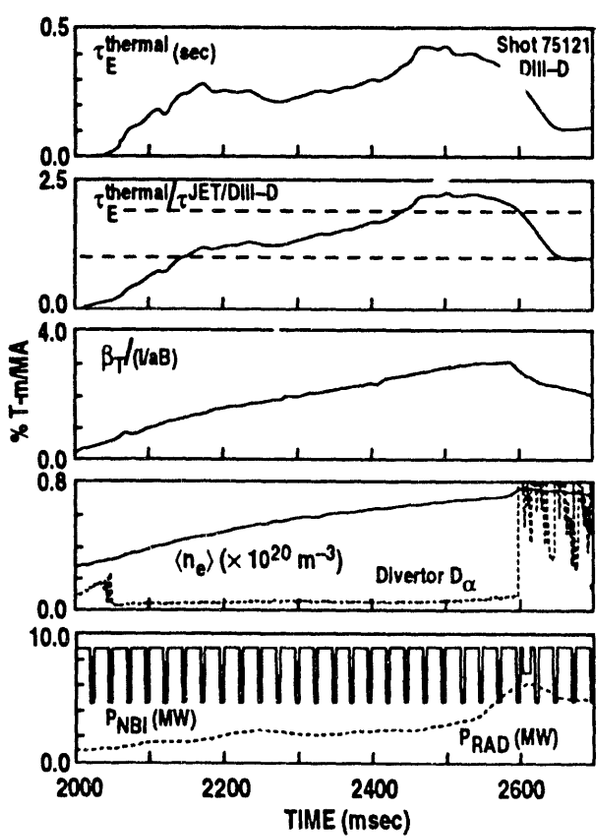

Figure 3. Time history of a VH-mode discharge in DIII-D, showing thermal confinement time $\tau_E^{thermal}$, confinement enhancement factor $\tau_E^{thermal}/\tau_E^{JET/DIII-D}$, normalized toroidal beta $\beta_T/(I_P/aB_T)$, line averaged electron density $\langle n_e \rangle$, recycling light from the divertor D_α, injected neutral beam power P_{inj}, and radiated power P_{rad} (shot 75121, DND, I_P = 1.6 MA, B_T = 2.1 T, P_{NBI} = 8 MW).

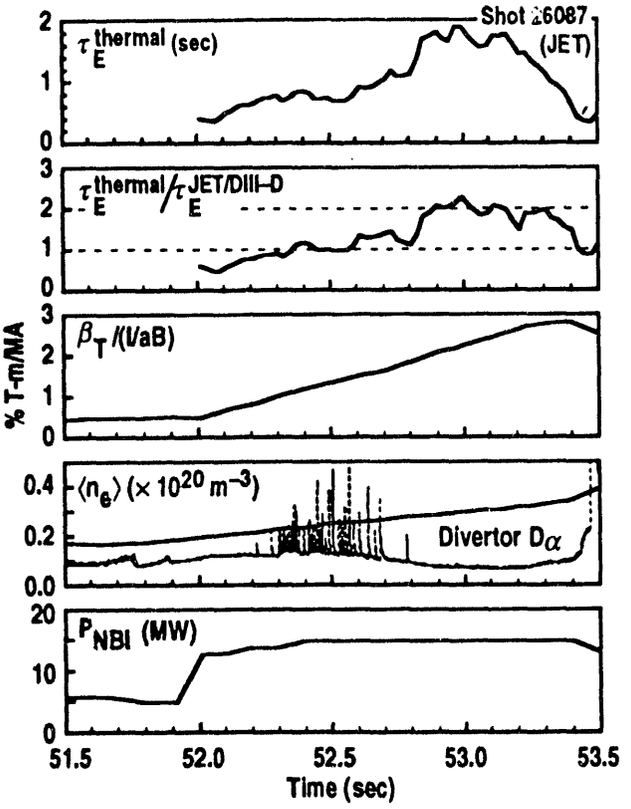

Figure 4. Time history of a VH-mode discharge in JET, showing thermal confinement time $\tau_E^{thermal}$, confinement enhancement factor $\tau_E^{thermal}/\tau_E^{JET/DIII-D}$, normalized toroidal beta $B_T/(I_P/aB_T)$, recycling light from the divertor D_α, and injected neutral beam power P_{inj} (shot 26087, SND, $I_P = 3.2$ MA, $B_T = 2.9$ T, $P_{NBI} = 14.6$ MW).

from H- to VH-mode, takes place during this ELM-free period. This transition corresponds to the reduction or elimination of MTEs (Osborne *et al.*, 1993), which are visible in data from FIR scattering, as well as in soft x-ray measurements at the same location. This will be discussed in more detail in section 3.

In JET (figure 4), the plasma is held in a limiter configuration until the desired time for the L–H transition. This allows for a long L-mode phase with significant power. At 51.0 sec, the plasma is diverted and the input power is increased. An L–H transition follows, which in turn is quickly followed by the beginning of an ELMing phase. The transition to the VH-mode phase occurs at the time the ELMs stop. In a recent experiment in DIII-D, this behavior was at least partially duplicated by mimicking the JET recipe of a long, high power L-mode phase prior to the H-mode (figure 5). The rather low peak confinement in this discharge may be explained by the fact that at the H–VH transition, the discharge had already reached a rather high normalized beta and underwent an early MHD event.

The improved confinement in VH-mode corresponds to a broadening of the regions of high density and temperature gradients which develop near the edge during H-mode (figure 6). In DIII-D, the transition is marked by a "spinup" in the toroidal plasma velocity in the plasma interior, and the elimination of a flattening of the toroidal rotation profile at normalized radius $0.6 < \rho < 0.8$. The ion temperature gradient exhibits a similar increase. Transport analysis has been carried out using ONETWO (Pfeiffer *et al.*, 1985) for the DIII-D discharges, and TRANSP (Goldston *et al.*, 1981) for the JET discharges. In DIII-D (figure 7), the single fluid heat diffusivity χ_{eff} decreases over the entire ELM-free period, while the angular momentum diffusivity $\chi_{ANG-MTM}$ undergoes a rapid decrease at the H–VH transition. The region where this decrease is most pronounced corresponds to the flattening of the rotation profile observed in figure 6(a). In JET (figure 8), the improvement in ion thermal diffusivity χ_i occurs first in the interior of the plasma, prior to the ELMing phase. Here, $\chi_{ANG-MTM}$ is low at all times during the H- and VH-mode, with some slight reduction over time. There is no feature observed

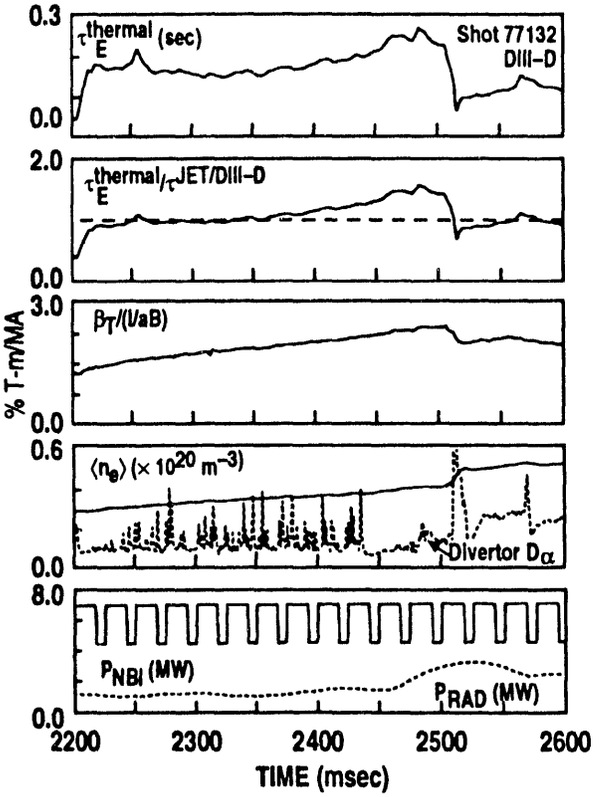

Figure 5. A DIII-D discharge with a similar shape and program to the JET discharge behaves in a similar manner to the JET discharge. The VH-mode phase terminates early due to the high normalized beta already attained during the ELMing phase (shot 77132, SND, I_P = 1.4 MA, B_T = 2.1 T, P_{NBI} = 6.5 MW).

corresponding to the flattening of the rotation profile in DIII-D. CXRS measurements from which the rotation is determined have a radial resolution of 10 to 15 cm, defining an upper limit to any such flattening.

Another characteristic of the VH-mode discharges is a large bootstrap current density which develops near the plasma edge in both devices. This current can be important in obtaining the VH-mode by opening access to the second stable regime to ideal ballooning modes (see section 3).

After the VH-mode begins, the behavior of plasmas in the two devices is quite similar. Confinement increases by as much as a factor of two or more over the time period of hundreds of milliseconds. In most of these discharges, the high performance phase is terminated by an MHD event which is related to high beta and high edge current (due to the aforementioned bootstrap current). At the time of this event, energy is rapidly lost from the entire plasma. In most cases, this is followed by an ELMing H-mode phase, and the high performance is usually not recovered (there have been several instances of discharges which appear to recover after the event in DIII-D). In discharges which do not undergo this event, confinement flattens and remains roughly constant at around twice that of H-mode.

Except where otherwise noted, the expression "thermal confinement time" refers here to

$$\tau_E^{thermal} = \frac{W_{MHD} - W_{FFORM} - 0.75\,W_{FICRH}}{P_{OHM} + P_{AUX} - (dW_{MHD}/dt)} \quad ,$$

which is that used for the ITER H-mode database work (ITER H-mode Database Working Group, 1993). In this expression, W_{FFORM} refers to the total fast ion energy due to neutral beam injection estimated from an approximate formula (where we have plotted time histories of thermal confinement time from JET, the fast ion energy is estimated by TRANSP rather than by the approximate formula), and W_{FICRH} to the perpendicular fast ion energy content during ICRH heating as estimated by the PION (Eriksson *et al.*, 1993) code. Although none of the

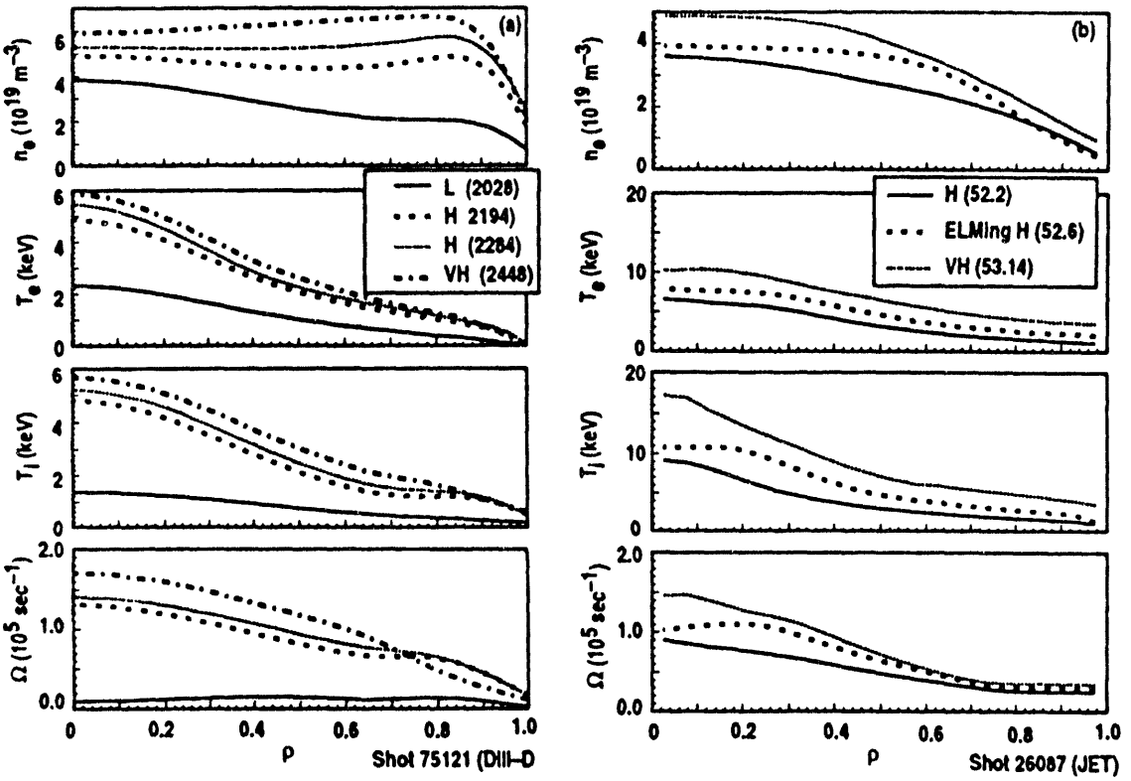

Figure 6. (a) Profiles of electron density n_e, electron and ion temperatures T_e and T_i, and toroidal rotation speed W during the L, H, and VH-mode phases of a discharge in DIII-D (Shot 75121, DND, I_P = 1.6 MA, B_T = 2.1 T, P_{NBI} = 8 MW). (b) The same profiles in JET, early in the H-mode phase, during the ELMs and in the VH-mode phase (shot 26087, SND, I_P = 3.2 MA, B_T = 2.9 T, P_{NBI} = 14.6 MW).

DIII-D VH-modes have ICRH, several of the JET VH-mode discharges are either partially or fully ICRH heated. Note that this expression does not fully include energy stored in plasma rotational momentum, which can be significant (on the order of 10% of the total) in some VH-mode plasmas.

3. Causes of enhanced confinement

Two factors have been identified which affect the improved confinement in VH-mode discharges. The first is the stabilization of turbulence by shear in the radial electric field (Osborne *et al.*, 1993; Burrell *et al.*, 1993). The second factor is expansion of the region in the plasma edge which has access to the second stable regime for ideal ballooning modes. These two effects appear to both be necessary for the enhanced confinement; the second stable edge allows the plasma to develop the steep core gradients inherent to high confinement.

3.1. Stabilization of turbulence by sheared $\vec{E} \times \vec{B}$ velocity

At the H-VH transition in DIII-D, the single fluid diffusivity χ_{eff} is reduced in the region $0.6 < \rho < 0.9$ (figure 7). One possible explanation for this behavior is the broadening of a region of high shear in the $\vec{E} \times \vec{B}$ velocity (Burrell *et al.*, 1993). This effect has previously been shown to be responsible for the development of the transport barrier near the plasma edge at the L-H transition (Burrell *et al.*, 1992).

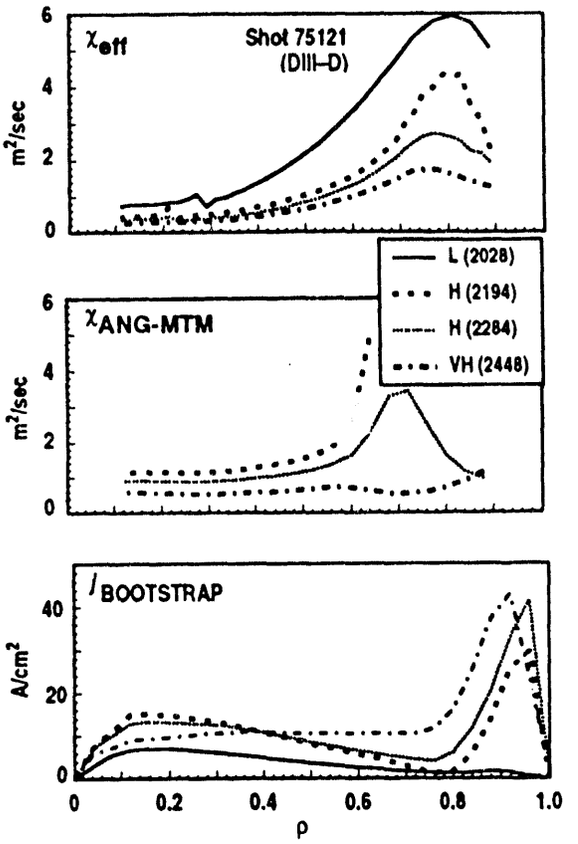

Figure 7. (a) In a discharge in DIII-D, the single fluid diffusivity χ_{eff} is reduced during the ELM-free period. (b) The reduction in the angular momentum diffusivity $\chi_{ANG-MTM}$ occurs much more rapidly, at the time of the H-VH transition. (c) The region where a large bootstrap current flows near the plasma boundary broadens during the ELM-free period (shot 75121, DND, I_P = 1.6 MA, B_T = 2.1 T, P_{NBI} = 8 MW).

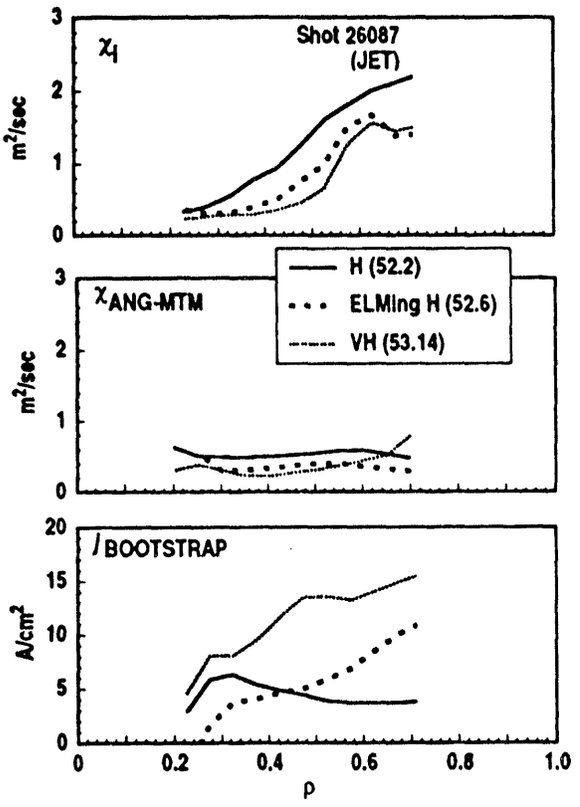

Figure 8. (a) In a discharge in JET, the ion thermal diffusivity χ_i in the interior of the plasma is reduced before the ELMing phase begins. (b) The angular momentum diffusivity $\chi_{ANG-MTM}$ steadily decreases during the entire H- and VH-mode phases. (c) The bootstrap current, especially in the outer regions of the plasma, grows throughout the H- and VH-mode phases (shot 26087, SND, I_P = 3.2 MA, B_T = 2.9 T, P_{NBI} = 14.6 MW). Note that the TRANSP results are of questionable validity outside of $\rho \approx 0.7$.

The radial electric field (inferred from charge exchange recombination measurements and the radial force balance equation) during the H-mode at 2140 msec (figure 9) has a region of strong shear extending from $\rho \approx 0.9$ to the edge. By 2490 msec, the shear region extends inward to $\rho \approx 0.6$. The region where we had already calculated improved transport quality (figure 7) corresponds to the newly developed E_r shear. The increased shear can be more directly perceived by the increase in toroidal velocity shear observed at $0.67 < \rho < 0.82$ (figure 9), beginning at about 2350 msec. Note that at the time of the "spinup," the toroidal velocity outside of the improved shear region actually decreases. It has also been observed that the "spinup" occurs before the improvement in the thermal transport (Burrell *et al.*, 1993), suggesting that the improved high shear in the $\vec{E} \times \vec{B}$ velocity may be the cause of the improved confinement, rather than a consequence of it.

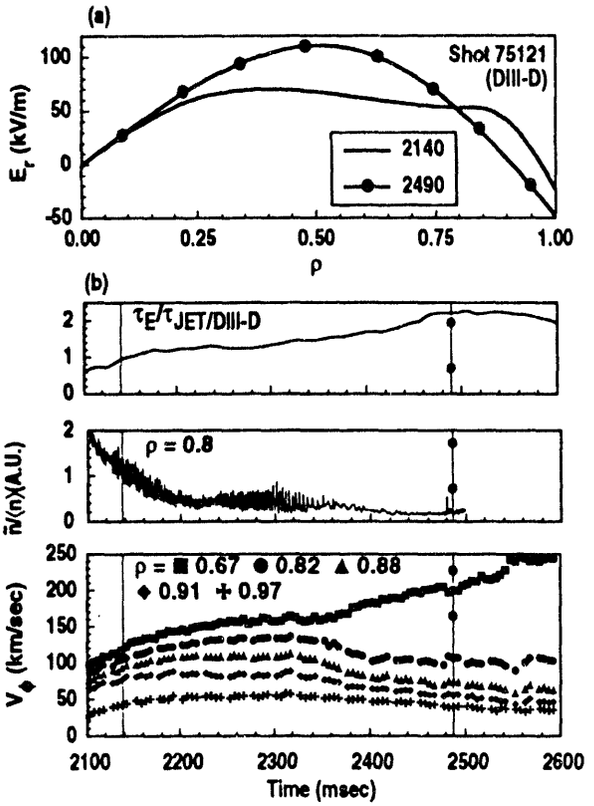

Figure 9. (a) Profiles of the radial electric field during the H- and VH-mode phases of a discharge in DIII-D. (b) Time histories of confinement enhancement, electron density fluctuations, integrated over the 0.5 to 1.5 MHz range, at $\rho \approx 0.8$ (FIR scattering), and toroidal rotation at several radial locations (shot 75121, DND, $I_P = 1.6$ MA, $B_T = 2.1$ T, $P_{NBI} = 8$ MW).

In order to predict the impact of the improved velocity shear, observations have been compared to the Biglari, Diamond and Terry (1990) expression for the magnitude of shear necessary for turbulence suppression (Osborne *et al.*, 1993; Burrell *et al.*, 1992). According to the theory, the measured shear should be adequate to suppress fluctuations in the discharge shown in figure 9 over most of the region where improved thermal transport is found. Density fluctuations, detected primarily by FIR scattering measurements (Rettig, 1992) are indeed seen around $\rho \approx 0.8$ during the H-mode phase of the discharge (figure 9). The fluctuations, in the 0.5 to 1.5 MHz range, occur in short repetitive bursts, which slow and usually completely cease at about the same time as the "spinup" in the toroidal rotation velocity begins. Because the increased velocity shear is associated with the disappearance of these bursting density fluctuations, the bursts have been dubbed momentum transfer events, or MTEs (Burrell *et al.*, 1992). The MTEs have also been observed in soft x-ray and magnetic probe measurements of MHD mode rotation frequency.

In JET, there is no direct evidence that shear suppression of turbulence is responsible for the improved confinement and further studies are being undertaken. However, it is observed that in two similar discharges, one of which obtains VH-mode and one which does not, there is drastically different behavior in the toroidal rotation (figure 10). In the discharge which obtains VH-mode (26087), the toroidal rotation and its shear increases continuously throughout the plasma cross-section. As previously mentioned, no flattening of the toroidal rotation profile is observed, setting an upper limit to the size of a possible unobserved "flat spot" of 10 to 15 cm. The lack of a "flat spot" may not be surprising, since no MTEs have been observed in JET discharges. Although there is no event apparent in the velocity shear formation which correlates to the relatively sudden transition to VH-mode, there does appear to be a correlation between a gradual global velocity shear improvement and the existence of a transition. It should also be noted that in the "JET-like" DIII-D case (figure 5), there was also no observation of MTEs or a flattening of the rotation profile. The toroidal rotation in this discharge behaves in a very similar manner to the JET discharge. In the JET discharge which remains in H-mode (25432), the toroidal rotation and its shear through most of the plasma cross-section drop continuously during the H-mode phase, following an initial rise after the L-H transition (figure 10; there are no ELMs in this discharge during the time shown in the figure).

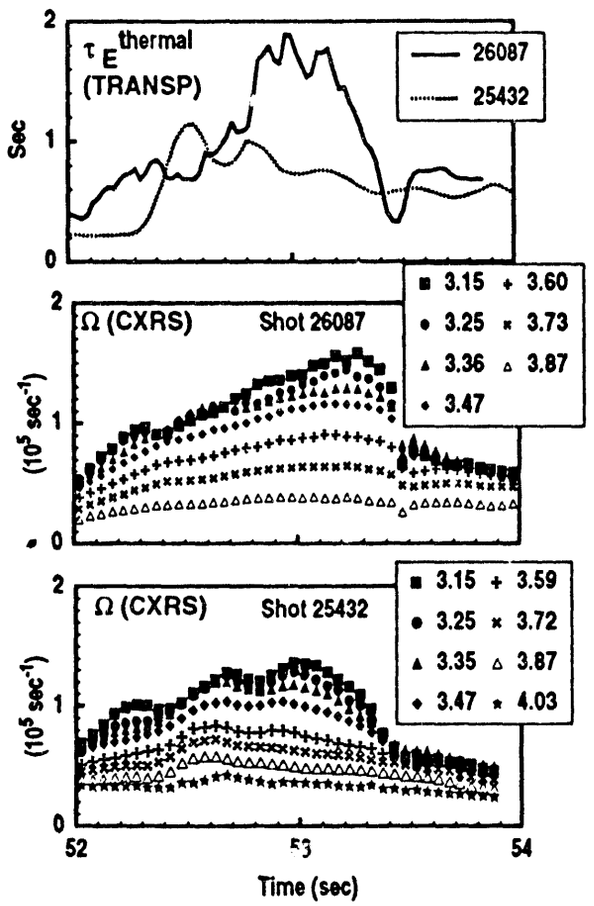

Figure 10. Time histories of two JET discharges: shot 26087 (SND, I_P = 3.2 MA, B_T = 2.9 T, P_{NBI} = 14.6 MW), which obtains VH-mode, and shot 25432 (DND, I_P = 3.1 MA, B_T = 2.9 T, P_{NBI} = 15.6 MW, timebase advanced by 1.0 sec), which does not. The discharge which obtains VH-mode is characterized by toroidal rotation which is increasing every-where in the plasma during the H- and VH-mode phases. In contrast, the discharge which remains in H-mode exhibits toroidal rotation which decreases everywhere along with the confinement time. The toroidal rotation is plotted at different major radii, as indicated. The magnetic axis is at $R \approx 3.1$ m and the plasma edge is at $R \approx 4.1$ m.

3.2. Access to the second stable regime to ideal ballooning modes

In discharges in both devices, high levels of bootstrap current are calculated near the plasma edge. Calculations in JET discharges indicate that a portion of the plasma edge gains access

to the second stable regime at about the time the ELMing phase ends (Deliyanakis *et al.*, 1993) (figure 11). For these calculations, kinetic profiles near the edge were generated using the microwave reflectometer (for electron density) and heterodyne radiometer (for electron temperature) diagnostics. A code has been written which uses these data, in addition to an equilibrium generated from magnetics data by IDENTC (Blum *et al.*, 1990) or EFIT (O'Brien *et al.*, 1992), to solve the ideal (non-resistive) ballooning equation (Bishop, 1986) as a function of normalized current density Λ and normalized pressure gradient α.

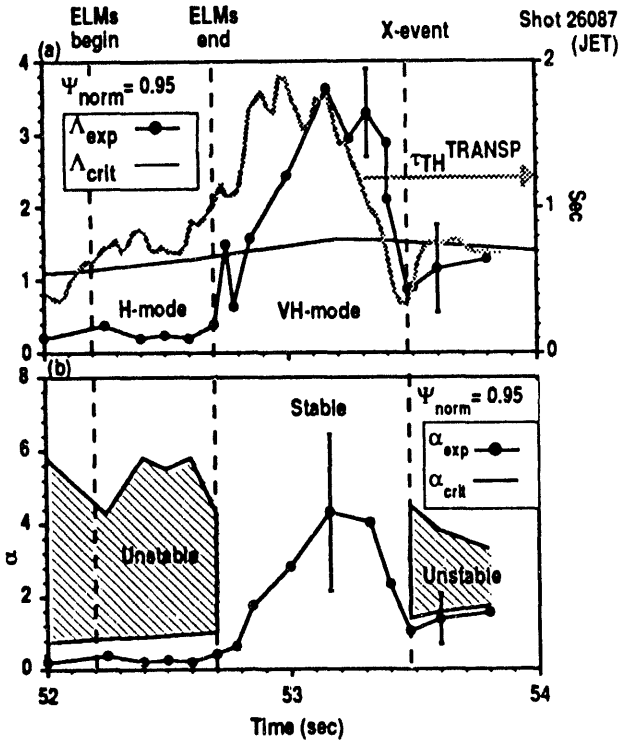

Figure 11. (a) At the transition to VH–mode in a JET discharge, the value of Λ_{exp} (normalized current density) exceeds the critical value Λ_{crit}, implying access to the second stable regime to ideal ballooning modes at $\Psi_{norm} = 0.95$. (b) At the same time, the first and second regimes (as indicated by the regions of stable α, or normalized pressure gradient) coalesce as the second regime is accessed. Access to the second regime is lost at about the time of the termination event (shot 26087, SND, $I_P = 3.2$ MA, $B_T = 2.9$ T, $P_{NBI} = 14.6$ MW). Note that the accuracy of profile measurements is reduced during the ELMs between 52.2 and 52.7 sec.

In figure 11(a), we see that at the time of the transition to VH–mode, the normalized current density Λ_{exp} inferred from the experimental data at $\Psi_{norm} = 0.95$ (the flux surface where poloidal flux is 95% of the edge value) exceeds the critical value Λ_{crit}, indicating coalescence of the first and second regimes. In other words, at the measured current density, there is no pressure gradient at which the plasma is unstable to ideal ballooning modes [figure 11(b)]. It has also been observed that the region with access to the second stable regime increases with time, in some cases reaching over 30% of the plasma volume (Deliyanakis *et al.*, 1993). The time of access to the second regime coincides with the termination of the ELMs. In all of the JET discharges studied, it is apparent that the transition to VH–mode occurs only when access to the second regime is obtained near the edge. This contrasts with the situation in the "standard" DIII–D configuration.

An infinite n, ideal ballooning mode stability calculation was performed for the DIII–D discharges using the CAMINO (Chance, 1987) code. In the "standard" DIII–D configuration, a large portion of the plasma volume naturally accesses the second regime, by virtue of its favorable shape (Jackson *et al.*, 1992; Greenfield *et al.*, 1992; Taylor *et al.*, 1993; Osborne *et al.*, 1993) (figure 12). Based on this information, second regime access cannot be ruled out as a necessary condition, but it is not a sufficient condition for the VH–mode transition to occur. In a typical VH–mode discharge, the plasma accesses the second stable regime only in the region between $\rho \approx 0.85$ and the edge (figure 12), while the decrease in thermal diffusivity is observed mainly in $0.6 < \rho < 0.9$ (figure 7). Unlike the paradigm of stabilization of turbulence

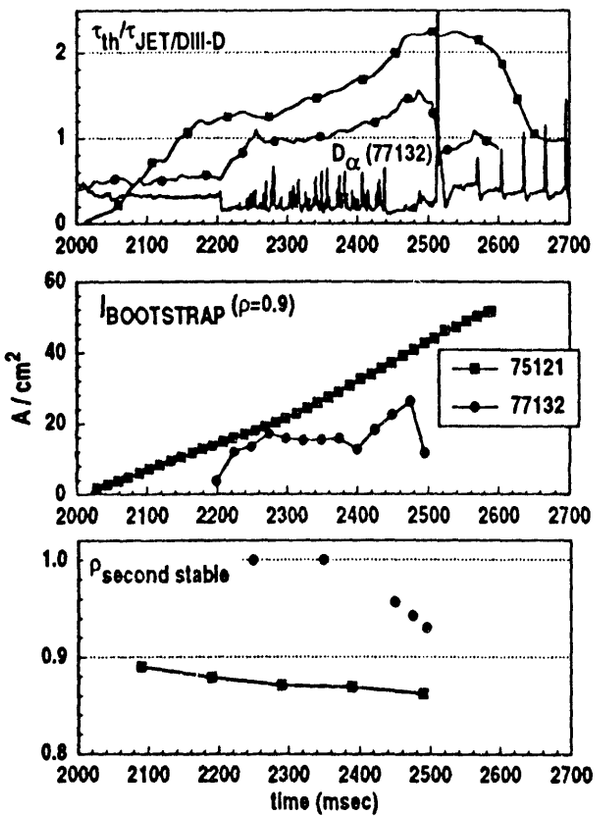

Figure 12. In a DIII–D discharge with the "normal" VH–mode configuration (shot 75121, DND, I_P = 1.6 MA, B_T = 2.1 T, P_{NBI} = 8 MW), the normalized radial position $\rho_{second\ stable}$ outside of which the second regime is accessed is relatively constant, despite the steadily growing bootstrap current near the edge. In a discharge where we attempted to emulate the JET discharges (shot 77132, SND, I_P = 1.4 MA, B_T = 2.1 T, P_{NBI} = 6.5 MW), the second stable regime is accessed at approximately the time the ELMing phases ends, shortly after the bootstrap current near the edge begins to grow.

by sheared $\vec{E} \times \vec{B}$ velocity, the volume of plasma which is affected by second stable regime access does not correspond to the region where the transport is improved, nor does this volume change appreciably while the confinement rises by a factor of two. Therefore, it is unlikely that the second regime access could be directly responsible for the confinement improvement.

When this analysis is performed on the "JET-like" discharge (77132, figure 12), the results are in agreement with those obtained in JET. Second stable access is obtained at the edge near the termination of the ELMing period. The region with access to the second regime grows inward until the MHD event which terminates the high confinement phase of the discharge. In this discharge, as in the JET discharges, the primary importance of the second regime access could very well be the avoidance of ELMs. The ELMs may impede the growth of the radial electric field shear, especially near the edge, thus preventing the VH–mode from developing. Exactly how these effects interplay with one another is under further study.

4. Termination of the High Performance Phase

In both DIII–D and JET discharges, the high performance phase is often terminated by a global MHD event which can result in a prompt (100 to 300 μsec) loss of a substantial amount of the plasma energy across the entire plasma (Greenfield *et al.*, 1992; Osborne *et al.*, 1993; Balet *et al.*, 1993; Strait *et al.*, 1993; Nave *et al.*, 1993). An example of a VH–mode termination in DIII–D is shown in figure 13. The plasma energy continues to rise until the MHD event occurs. The MHD event is initiated by a rapidly growing ($\sim$ 20 to 50 μsec) mode with toroidal mode number $n \approx 3$ to 5. A growing internal $m = 1$, $n = 1$ mode [see figure 13(a)] is often observed before the rapid growth of the $n \approx 3$ to 5. The rapid loss of energy is shown by the abrupt drop in the soft x–ray emission from the center to the edge [figure 13(b)]. In discharges where the $n = 1$ mode is not observed, there is an immediate loss of energy from the edge, but a slower loss from the center (Strait *et al.*, 1993). Following the termination event, the

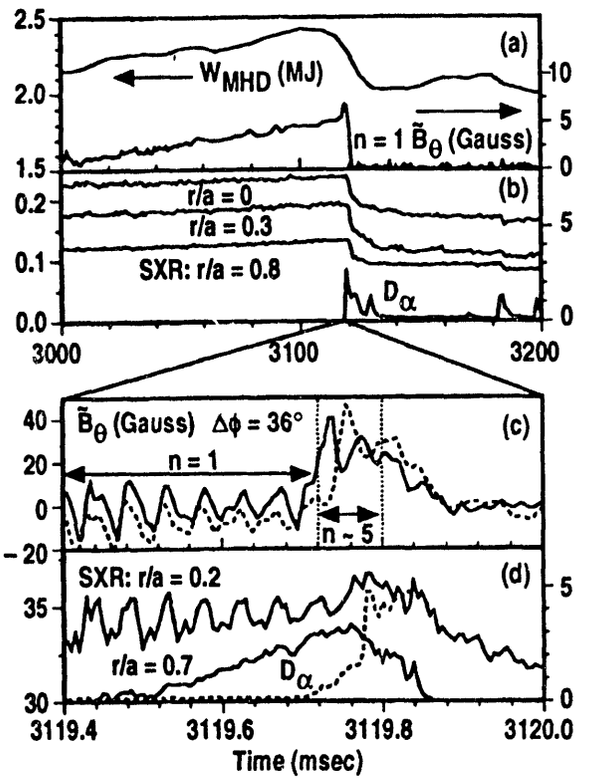

Figure 13. Time evolution of the MHD event terminating the VH-mode phase of a discharge in DIII-D (shot 73203, DND, I_P = 1.6 MA, B_T = 2.1 T, P_{NBI} = 10.75 MW). An internal mode with $(m,n) = (1,1)$ precedes the rapidly growing $n \approx 3$ to 5 mode near the surface. Energy is lost rapidly across the entire cross-section at the MHD event.

confinement time returns to that predicted by JET/DIII-D scaling. The precise cause of the termination event in JET is less clear. In some shots there is evidence for the involvement of the $n = 1$ mode in the collapse phase (Nave *et al.*, 1993). A detailed paper describing the termination event in JET is in preparation (Reichle *et al.*, 1993).

These experimental observations are consistent with ideal kink mode stability calculations. Stability of the free boundary $n = 1$ kink mode was calculated numerically for JET discharges using the CASTOR code (Kerner *et al.*, 1991). The calculations indicate that the $n = 1$ mode, which is normally an internal mode at low beta, has a significant edge component as beta or edge current density is increased (Nave *et al.*, 1993). The more global nature of this MHD mode at high beta might account for the observed prompt energy loss. The ideal stability of DIII-D discharges were evaluated with the GATO code (Bernard *et al.*, 1981). Just before the VH-mode termination, edge-localized kink modes with $n > 1$ are found to be unstable, while the $n = 1$ mode is only marginally stable. It is found that both the high edge pressure gradient and the high edge bootstrap current are destabilizing to $n = 1$, 2, and 3 ideal kinks (Strait *et al.*, 1993).

In both JET and DIII-D, these low n MHD modes are destabilized by high beta and high edge current density. Some success has been achieved in delaying the termination event in DIII-D by limiting beta by feedback control of the neutral beam input power. But, the beta limit is reduced as a consequence of growing edge bootstrap current. In JET, low power discharges which do not attain large beta have obtained nearly steady state high confinement.

It is clear that the factor which most limits the confinement here is MHD stability. Theoretical modeling predicts that if this limitation were removed, further improvements in confinement might be realized as the region of improved transport continues to penetrate the plasma (Staebler *et al.*, 1993).

Two possible methods which have been considered in DIII-D to reduce and control the edge bootstrap current in order to obtain higher beta high performance discharges are (1) the addition of impurities to radiatively cool the edge and (2) the use of counter lower hybrid

current drive. However, the edge current density also provides access to the second regime of stability and increases the region of second regime access, and may be needed for the improved confinement. In DIII-D, discharges where a strong negative current ramp has been used to substantially reduce the edge current density, the VH-mode has not yet been obtained (Taylor *et al.*, 1993).

5. Summary

The VH-mode regime of high confinement has now been studied in two devices, in different configurations and with different heating methods: JET (low to moderate triangularity SND and DND, with NBI and/or ICRH) and DIII-D (high and low triangularity SND and DND, all with NBI). Although the temporal sequence of events leading up to the VH-mode differs between the two machines, the resulting situation is quite similar: the VH-mode is characterized by high density and temperature gradients, which extend much deeper into the plasma than in H-mode. Both thermal and momentum confinement is seen to be improved over H-mode, resulting in confinement on the order of twice that in H-mode.

It appears that there are two necessary conditions to obtain improved confinement. Neither by itself is a sufficient condition for development of VH-mode. The first is access of the plasma edge to the second stability regime for ideal ballooning modes. The primary importance here seems to be the avoidance of ELMs which inhibit the transition to VH-mode. The second condition is the extension of the radial electric field gradient toward the plasma core, which is known to suppress fluctuations, thereby decreasing turbulent transport.

The differences between the JET and DIII-D discharges are mainly rooted in which of the above conditions is the critical one. In JET, the first condition, second regime access, seems to be the "trigger" for VH-mode. In DIII-D, the plasma edge is almost always in the second regime, so the second condition, radial electric field shear, becomes the "trigger." In a DIII-D discharge which emulates the JET shape and shot program, the JET behavior is reproduced.

The high performance phase of both devices is usually limited by a global MHD event which is sensitive to both beta and edge current density. Some success has been achieved in avoiding this event, but this has mostly been at the expense of performance. Work with active control of plasma parameters to avoid the MHD event and improve performance is ongoing.

Acknowledgments

This joint effort between the DIII-D and JET Teams was carried out under an "Agreement for Cooperation between the European Atomic Energy Community and the United States Department of Energy in the Field of Controlled Thermonuclear Fusion." The work of the DIII-D Team was sponsored by the U.S. Department of Energy under Contract DE-AC03-89ER51114 and Grants DE-FG03-92ER54150 and DE-FG03-86ER-52126.

References

Balet B, Stubberfield P M, Borba B *et al.* 1993 JET Report JET-P(93)18, submitted to *Nucl. Fusion.*

Bernard L C *et al.* 1981 *Comput. Phys. Commun.*, **24**, 377.

Biglari H, Diamond P H and Terry P W 1990 Phys. Fluids B **2**, 1.

Bishop C M 1986 *Nucl. Fusion* **26**, 1063.

Blum J, Lazzaro E, O'Rourke J *et al.* 1990 *Nucl. Fusion* **30**, 1475.

Burrell K H, Osborne T H, Groebner R J and Rettig C L 1993 General Atomics Report GA-A21308, this conference.

Burrell K H, Carlstrom T N, Doyle E J *et al.* 1992 *Plasma Phys. and Contr. Fusion Res.*, **34**, 1859.

Chance M S 1987 *Proceedings of Theory of Fusion Plasmas*, Varenna, Italy, p. 87.

Deliyanakis N, Balet B, Greenfield C M *et al.* 1993 JET Report JET-P(93)37, this conference.
Eriksson L G, Hellston T and Willen U, submitted to Nucl. Fusion.
Goldston R J, McCune D C, Towner H H *et al.* 1981 *J. Comput. Phys.* **43**, 61.
Greenfield G M, Jackson G L, Burrell K H *et al.* 1992 *Controlled Fusion and Plasma Physics*, European Physical Society, Petit-Lancy, 1992, Vol. 16C, Part I, p. 11.
ITER H-mode Database Working Group, to be submitted to *Nucl. Fusion.*
Jackson G L, Winter J, Taylor T S *et al.* 1991 *Phys. Rev. Lett.* **67**, 3098.
Jackson G L, Winter J, Taylor T S *et al.* 1992 *Phys. Fluids B* **4**, 2181.
Kerner W *et al.* 1991 *Controlled Fusion and Plasma Physics*, European Physical Society, Petit-Lancy, 1991, Vol. IV, p. 98.
Nave M F F, deBlank H J, Borba D *et al.* 1993 JET Report JET-P(93)37, this conference.
O'Brien D P, Lao L L, Solano E R *et al.* 1992 *Nucl. Fusion* **32**, 1351.
Osborne T H, Burrell K H, Carlstrom T N *et al.* 1993 *General Atomics Report* GA-A21182, submitted to *Nucl. Fusion.*
Pfeiffer W, Marcus F B, Armentrout J C *et al.* 1985 *Nucl. Fusion* **25**, 655.
Reichle R, Campbell D, Arshad A *et al.*, in preparation.
Rettig C L 1992 *Ph.D. Thesis*, University of California at Los Angeles.
Schissel D P, DeBoo J C, Burrell K H *et al.* 1991 *Nucl. Fusion* **31**, 73.
Staebler G M, Hinton F L, Wiley J C *et al.* 1993 *General Atomics Report* GA-A21278, submitted to *Phys. Fluids B.*
Strait E J, Taylor T S, Turnbull A D *et al.* 1993 *General Atomics Report* GA-A21301, this conference.
Taylor T S, Osborne T H, Burrell K H, *et al.* 1993 *Plasma Physics and Controlled Nuclear Fusion Research*, International Atomic Energy Agency, Vienna, to be published, paper CN-56/A-3-1.
The JET Team 1989 *Plasma Physics and Controlled Nuclear Fusion Research*, International Atomic Energy Agency, Vienna, Vol. 1, p. 159.
The JET Team 1992 *Plasma Phys. and Contr. Fusion Res.*, **34**, 1749.
Yushmanov P N, Takizuka T, Riedel K S, *et al.* 1990 *Nucl. Fusion* **30**, 1999.

DATE
FILMED
9/28/94

END